LLC Resonant Converter with Wide Output Voltage Control Characteristics According to Operating Mode Transition

Eun-Soo Kim[1], Jicheol Lee[1], Yechang Heo[1], Takongmo Marius[1], Jongseong Ju[1], Yoon-Sang Kook[2]

[1]Electrical and Electronics Engineering Jeonju University, Jeonju, Republic of Korea, Email: eskim@jj.ac.kr

[2]PACTECH CO.,LTD., 8,72Beon-Gil, Deokcheon-Ro, Manan-Gu, Anyang-City, Republic of Korea

***Abstract*— This paper presents an LLC resonant converter which operates over a wide output voltage control characteristics by changing the operating modes of the switching devices. As the converter transits from one operating mode to the other, the primary and secondary terminals of the two transformers are either connected in parallel or the series and makes it possible to achieve a wide controllable output voltage (50V_{DC}- 800V_{DC}). Each mode is operated with a varying frequency (FM) and voltage/current over-shoots or under-shoots are minimized as the converter transits from one operating mode to the other. Moreover, a hysteresis control band is introduced between the operating modes to ensure stable mode transition. The feasibility of the proposed converter is verified with experimental results of a 2kW prototype.**

I. INTRODUCTION

Recently, various types of batteries have been used for electric forklifts, electric vehicles and electric buses and there is a demand for a charging system having a wide controllable output voltage range (50V_{DC}- 800V_{DC}) capable of charging these battery banks. In addition, with the aim of achieving high integration and high efficiency, LLC resonant converters operating at high switching frequencies with zero voltage and zero current switching (ZVS/ZCS) for all load condition had been researched [1]-[4]. However, LLC resonant converters can only achieve zero voltage switching (ZVS) with all loads within a narrow output voltage control range. In an attempt to solve this problem, an LLC converter with two resonant circuits and a bidirectional auxiliary switch connected across one of its resonant circuits was proposed [5]. Short-circuiting one of the resonant tanks with the auxiliary switch made it possible to control a wide output voltage but the converter suffered from conduction losses. Moreover, in [6]-[7] an LLC converter with the primary switches configured to operate in the full bridge and half bridge modes was proposed to control a wide output voltage. However, all the previously proposed converters can't provide a wide output voltage than 4V_o.

II. LLC RESONANT CONVERTER WITH A WIDE OUTPUT VOLTAGE CONTROL CHARACTERISTIC

With conventional LLC resonant converters, a wide controllable output voltage is achieved by designing the magnetizing inductance to be small; but it is difficult to operate conventional LLC converters with high efficiency within a very wide controllable output voltage range (50V_{DC}~800V_{DC}) [8]-[9]. The proposed converter provides high efficiencies with all loads thanks to the transition in operating modes. Figure 1 shows the schematic circuit of the proposed LLC converter and the gain characteristic curves of operating mode 0, mode 1, mode 2 and mode 3 [9].

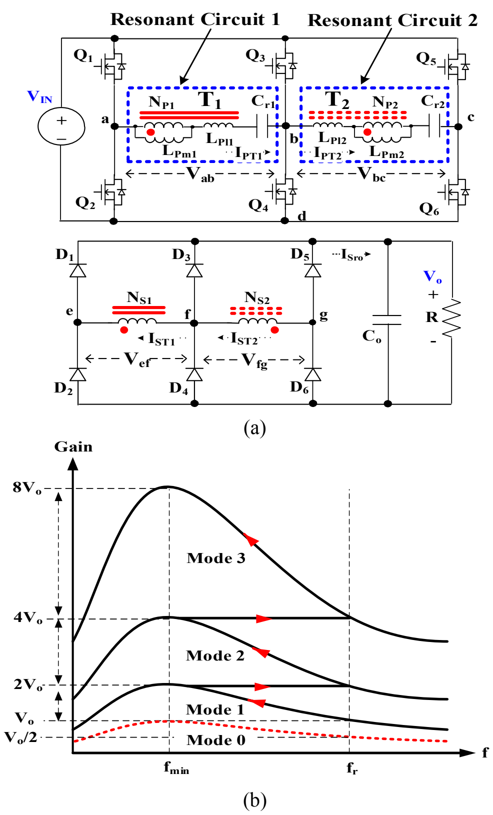

Figure 1. (a) Proposed 3-bridge LLC resonant converter and (b) voltage gain characteristics

In the proposed LLC resonant converter, the primary windings (N_{P1},N_{P2}) of the two transformers (T_1,T_2) and the resonant capacitors (C_{r1},C_{r2}) are connected to the switching elements (Q_1~Q_6) arranged in a three-bridge configuration as shown in

Figure 1(a). The secondary windings are connected to the output diodes (D_1-D_6) equally arranged in a three-bridge configuration. The proposed converter can operate in four different modes depending on the switching pattern of the switching devices (Q_1~Q_6). The voltage gain characteristic curves of each mode are shown in Figure 1(b). In each operating mode, the switching devices are switched with a variable frequency (FM: frequency modulation), moreover; operating mode transitions are done with slight voltage and current over/under shoots. The switching pattern of each operating mode is shown below.

In mode 0, the switching devices Q_1 and Q_2 are alternately switched with a 50% duty, Q_3, Q_4 and Q_5 are off while Q_6 is constantly on. As a result, the primary terminals of the resonant circuits (1&2) are connected in series while the secondary terminals are connected in parallel as shown in Figure 2. Mode 0 is a half bridge configuration, and 1/4 of the input voltage V_{in} is applied across the terminals of the LLC resonant circuits (1&2). The secondary windings (N_{S1} &N_{S2}) are connected in parallel across the output rectifying diodes (D_1-D_6) in accordance with the polarity of the secondary windings. The resonant currents (I_{ST1} & I_{ST2}) are rectified and power is transfer to the load. Figure 2 shows the circuit diagrams of the proposed converter operating in mode 0 and its operating waveforms.

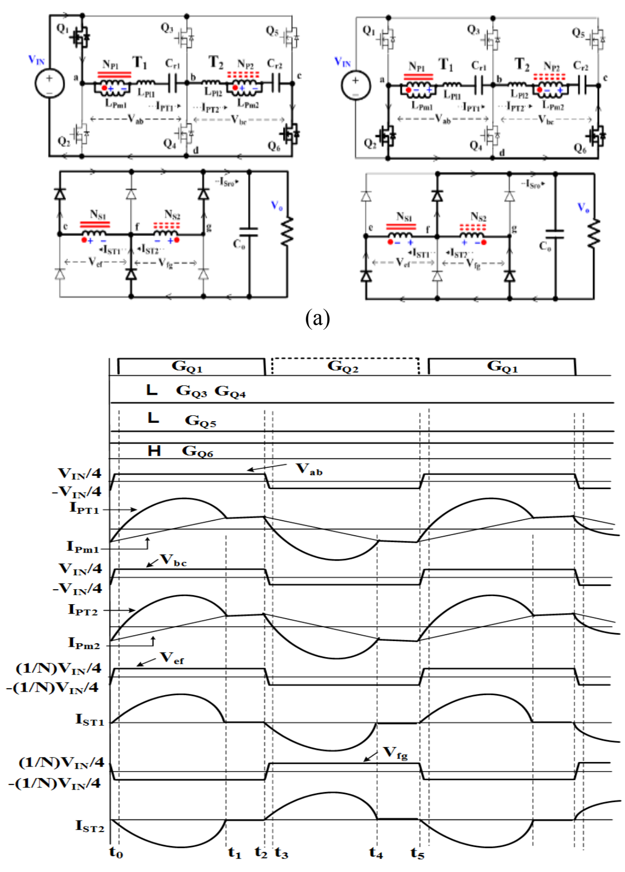

(a)

(b)

Figure 2. (a) Operating mode 0 and (b) its operating waveforms

In mode 1, the main switching devices Q_1 & Q_2 and Q_5 & Q_6 are alternately switched with 50% duty while Q_3 & Q_4 are constantly off. As Q_1 & Q_6 and Q_2 &Q_5 are simultaneously switched on / off, mode 1 operates in a full bridge configuration. The primary terminals of the resonance circuits (1&2) are connected in series and 1/2 of the input voltage (V_{in}) is applied across their terminals. Moreover, the secondary windings (N_{S1} & N_{S2}) are connected in parallel across the output rectifying diodes (D_1~ D_6) in accordance to the polarity of the secondary windings. The resonant currents (I_{ST1} & I_{ST2}) are rectified and power is transfer to the load. The circuit diagram of the proposed converter operating in mode 1 and its operating waveforms are shown in Figure 3.

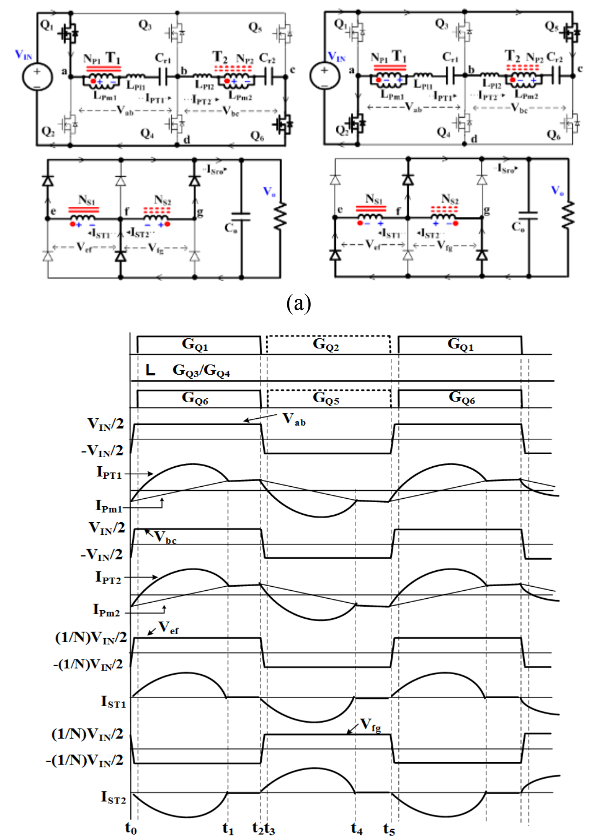

(a)

(b)

Figure 3. (a) Operating mode 1 and (b) its operating waveforms

In mode 2, the switching devices Q_1 & Q_2 and Q_5 & Q_6 are alternately switched with 50% duty, Q_3 is constantly off while Q_4 is on. Moreover, the switching devices Q_1 &Q_5 and Q_2 &Q_6 are simultaneously switched on/off as shown in Figure 4(a). A second switching pattern of mode 2 is shown in Figure 4(b): the switching device Q_3 and Q_4 are alternately switched with 50% duty, Q_1 & Q_5 are constantly switched off while Q_2 & Q_6 are on. As a result, the primary terminals of the resonant circuits (1&2) are connected in parallel while the secondary terminals are connected in series across the output rectifying diodes (D_1~D_6). Mode 2 operates in a half bridge configuration and

1/2 of the input voltage (V_{in}) is applied across the primary terminals of the resonant circuits. The output diodes (D_1~D_6) rectify the resonant currents (I_{ST1} & I_{ST2}) in the secondary terminals and power is transfer to the load. The circuit diagrams of the proposed converter operating in mode 2 and its operating waveforms are shown in Figure 4.

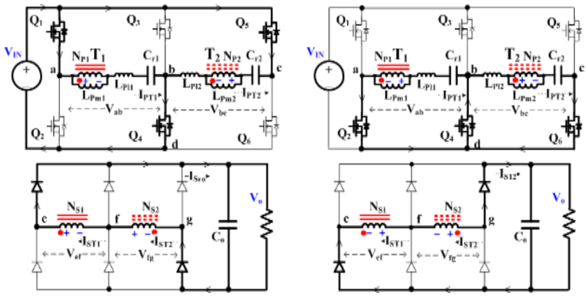

(a)

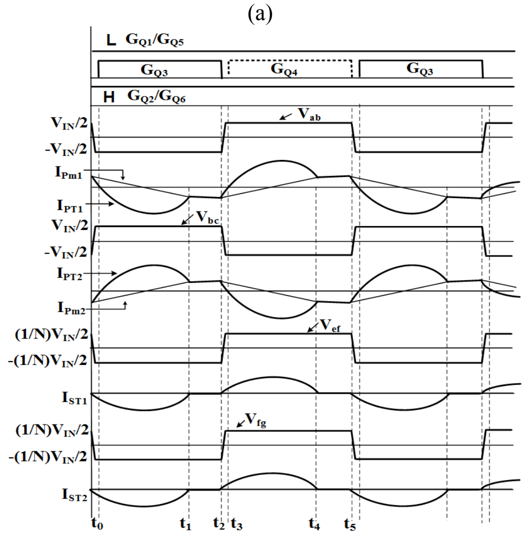

(b)

Figure 4. (a) Operating mode 2 and (b) its operating waveforms

In mode 3, the main switching devices Q_1 & Q_2, Q_3 & Q_4 and Q_5 & Q_6 are alternately switched with 50% duty. In addition, the switching switches Q_1,Q_4,Q_5 and Q_2,Q_3,Q_6 are simultaneously switched on or off. As a results, the primary terminals of the resonance circuits (1&2) are connected in parallel while the secondary terminals are connected in series across the bridge diodes (D_1~D_6).

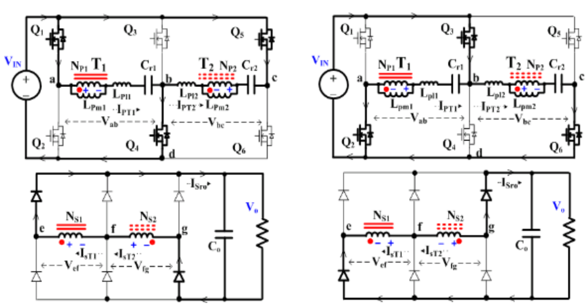

(a)

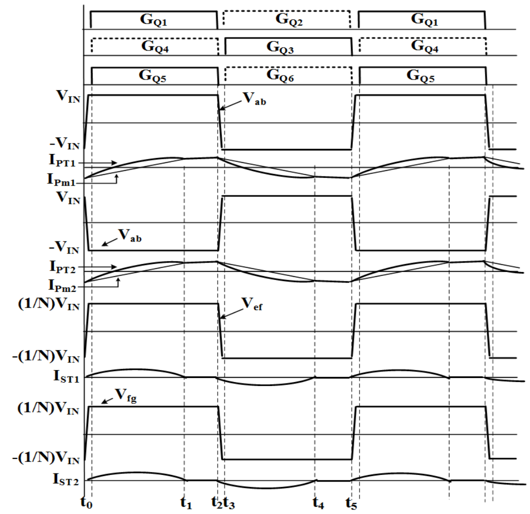

(b)

Figure 5. (a) Operating mode 3 and (b) its operating waveforms

Mode 3 operates in a full-bridge configuration, and the input voltage (V_{in}) is applied across the primary terminals of the resonant circuits (1&2). The resonant currents (I_{ST1} & I_{ST2}) are rectified and power is transfer to the load. The circuit diagrams of the proposed converter operating in mode 3 and its operating waveforms are shown in Figure 5.

III. THE VOLTAGE GAIN OF THE PROPOSED LLC CONVERTER

A. The voltage gain characteristics of mode 0 and mode 1

Figure (6) shows the equivalent circuit of mode 0 and 1. In mode 0 and mode 1, the primary terminals of resonant tank 1 and resonant tank 2 are connected in series while the secondary terminals are connected in parallel. This implies that the resonant capacitors (C_{r1} & C_{r1}), the primary leakage inductances (L_{P11} & L_{P12}) and the magnetizing inductances (L_{pm1} & L_{pm2}) are connected in series while the load resistors (N^2R_{ac1} & N^2R_{ac2}) and the secondary leakage inductances (N^2L_{S11} & N^2L_{S12}) as seen from the primary side are connected in parallel. The overall resonant frequency (f_r), equivalent leakage inductance (L_{eq}) and resonant capacitor (C_r) of these modes are expressed by the equations below.

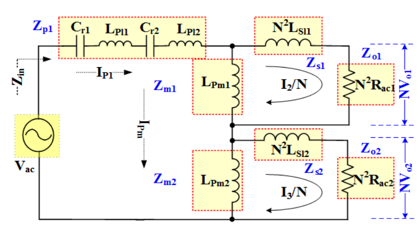

Figure 6. Equivalent circuit of mode 0 and mode 1

$$f_r = \frac{1}{2\pi\sqrt{L_{eq}C_r}},\ C_r = \frac{C_{r1}C_{r2}}{C_{r1}+C_{r2}} \tag{1}$$

$$L_{eq} = L_{pl1} + \frac{N^2L_{Sl1}L_{pm1}}{N^2L_{Sl1}+L_{pm1}} + L_{pl2} + \frac{N^2L_{Sl2}L_{pm2}}{N^2L_{Sl2}+L_{pm2}} \tag{2}$$

We assume that the two transformers have identical parameters, that is

$$L_{Pl1} = L_{Pl2},\ \ L_{Pm1} = L_{Pm2},\ \ C_{r1} = C_{r2},\ L_{Sl1} = L_{Sl2},$$
$$R_{ac1} = R_{ac2} \tag{3}$$

The normalize voltage gain ($G_{v0,1}$) for the resonant circuits is defined as

$$G_{v0,1} = \frac{1}{2\left(1 + A - \left(\frac{1}{\omega_n}\right)^2\left(A + \frac{B}{1+B}\right)\right) + j2Q(1+B)\left(\omega_n - \frac{1}{\omega_n}\right)} \tag{4}$$

Where

$$A = \frac{L_{Pl}}{L_m}, B = \frac{N^2 L_{Sl}}{L_{Pm}},\ Q = \frac{\omega_r L_{eq}}{N^2 R_{ac}} = \frac{1}{N^2 R_{ac}\omega_r C_r},\ \omega_n = \frac{\omega}{\omega_r},$$
$$L_{eq} = L_{Pm}\left(A + \frac{B}{1+B}\right)$$

Figure 7 shows the voltage gain characteristic curves of the proposed resonant converter operating in mode 0 and 1. Each operating mode is controlled with variable frequency (frequency modulation). When the proposed converter operates in mode 0, its output voltage ranges from $50V_{DC}$ to $100V_{DC}$ and its output ranges from $100V_{DC}$ to $200V_{DC}$, when its operates in mode 1.

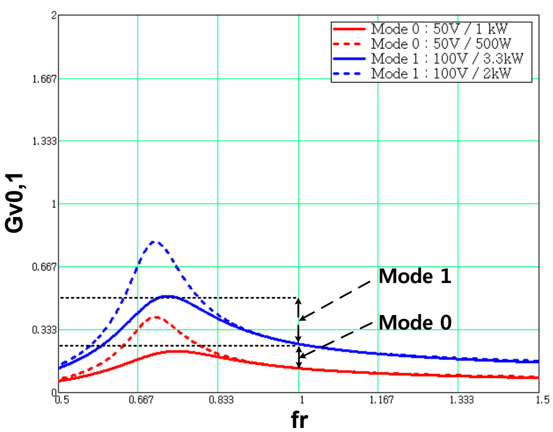

Figure 7. Voltage gain characteristic curve of mode 0 and mode 1

B. The voltage gain characteristics of mode 2 and mode 3

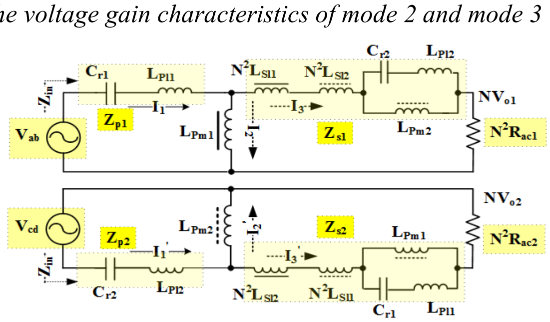

Figure 8. Equivalent circuits of mode 2 and mode 3

In mode 2 and 3, the primary terminals of resonant tank 1 and resonant tank 2 are connected in parallel while the secondary terminals are connected in series. The equivalent circuit of this mode is represented as a T-type circuit with two voltage sources (V_{ab}, V_{cd}). The overall gain ($G_{v2,3}$) of the converter operating in this mode is obtained through the superposition of the individual gains (G_{v2}, G_{v3}) of the voltage sources (V_{ab}, V_{cd}).

The voltage gain of V_{ab} source is defined as

$$G_{v2} = \frac{NV_{01}}{V_{ab}} \tag{5}$$
$$= \frac{1}{\left(1 + A_1 + \left(\frac{\omega_o}{\omega}\right)^2\left(1 + \frac{Z_{S1}}{N^2 R_{ac1}}\right)\right) + j\frac{\omega L_{Pm1}}{N^2 R_{ac1}}\left[\left(1 + A_1 - \left(\frac{\omega_o}{\omega}\right)^2\right)\left((B_1+1) - 1\right)\right]}$$

Also, the voltage gain of V_{cd} source is defined as

$$G_{v3} = \frac{NV_{01}}{V_{ab}} \tag{6}$$
$$= \frac{1}{\left(1 + A_2 + \left(\frac{\omega_o}{\omega}\right)^2\left(1 + \frac{Z_{S2}}{N^2 R_{ac1}}\right)\right) + j\frac{\omega L_{Pm2}}{N^2 R_{ac2}}\left[\left(1 + A_2 - \left(\frac{\omega_o}{\omega}\right)^2\right)\left((B_1+1) - 1\right)\right]}$$

Where

$$A_1 = \frac{L_{Pl1}}{L_{pm1}},\ B_1 = \frac{N^2 L_{Sl1}}{L_{pm1}},\ A_2 = \frac{L_{Pl2}}{L_{pm2}},\ B_2 = \frac{N^2 L_{Sl2}}{L_{pm2}},$$

$$G_{v2,3} = G_{v2} + G_{v3} \tag{7}$$

We assume that the two transformers have identical parameters, that is

$$L_{Pl1} = L_{Pl2}, L_{Pm1} = L_{Pm2}, C_{r1} = C_{r2}, L_{Sl1} = L_{Sl2},$$
$$R_{ac1} = R_{ac2} \tag{8}$$

The over voltage gain ($G_{v2,3}$) of the proposed converter is defined as

$$G_{v2,3} = \frac{1}{\left(1 + A - \left(\frac{1}{\omega_n}\right)^2\left(A + \frac{B}{1+B}\right)\right) + jQ_m\left(\frac{1}{N^2} + \frac{B}{N^2}\right)\left(\omega_n - \frac{1}{\omega_n}\right)} \tag{9}$$

Where,

$$A = \frac{L_{Pl}}{L_{pm}},\ \ B = \frac{N^2 L_{Sl}}{L_{pm}},\ \omega_n = \frac{\omega}{\omega_r},\ Q_m = \frac{\omega_r L_{eq}}{N^2 R_{ac}} = \frac{1}{N^2 R_{ac}\omega_r C_r}$$

Figure 8 shows the voltage gain characteristic curves of the proposed resonant converter operating in mode 2 and 3. Each mode operates with a varying frequency. When the proposed converter operates in mode 2, its output voltage ranges from $200V_{DC}$ to $400V_{DC}$ and its output ranges from $400V_{DC}$ to $800V_{DC}$, whenever its operates in mode 3.

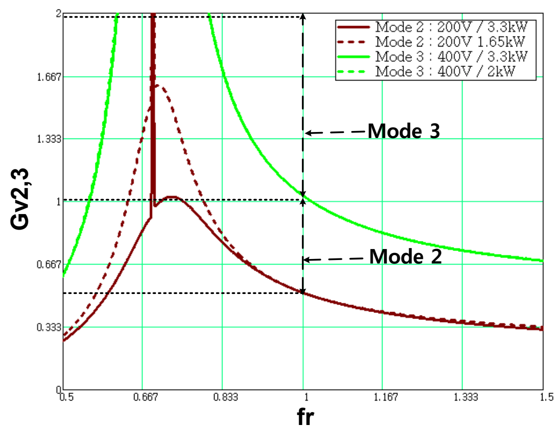

Figure 9. Voltage gain characteristic curve of mode 2 and mode 3

IV. EXPERIMENTAL RESULTS

Table. 1 Major ratings and transformer parameters

Major ratings	Input voltage(V_{in})	$400V_{DC}$	
	Output voltage(V_o)/ Output current(I_o)	$50V_{DC}/20A \sim 800V_{DC}/2.86A$	
Device	Switching element($Q_1 \sim Q_6$)	SCT3030AL (650V,70A,R_{DS}:30mΩ,SiC)	
	Output rectifier diode	GP2D050A120B (1200V,50A,V_F:1.6V,SiC	
Parameters	Resonant capacitor(C_{r1}, C_{r2})	$22nF/3000V_{DC}$	
	Resonance frequency(f_r)	138kHz	
Transformer (T_1/T_2)	Magnetizing inductance of the primary side	L_{P1}/L_{P2}	127.5uH/130.2uH
	Magnetic inductance of the secondary side	L_{S1}/L_{S2}	17.1uH/19.1uH
	Leakage inductance	Leq_1/Leq_2	61.32uH/60.28uH
	(Turn-ratio)	$n_1(N_{P1}/N_{S1})$/ $n_2(N_{P2}/N_{S2})$	3(24T/8T)

Table.1 shows the transformer parameters and the device ratings used in the proposed resonant converter. Figure 10 to Figure 13 show the primary/ secondary currents (I_{PT1} & I_{ST1}) and primary/ secondary voltages (V_{ab} & V_{ef}) across the terminals of resonant circuit 1.

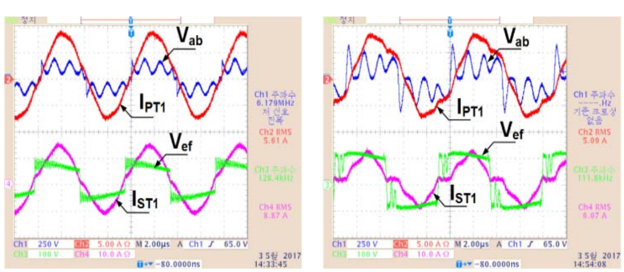

(a) Output ratings $50V_{DC}$/900W, (b) Output ratings $90V_{DC}$/900W
(ch1:250V/Div., ch2:5A/Div., ch3:100V/Div., ch4:10A/Div., 2us/Div.)
Figure10. Experimental waveforms of mode 0 ($50V_{DC} \sim 90V_{DC}$)

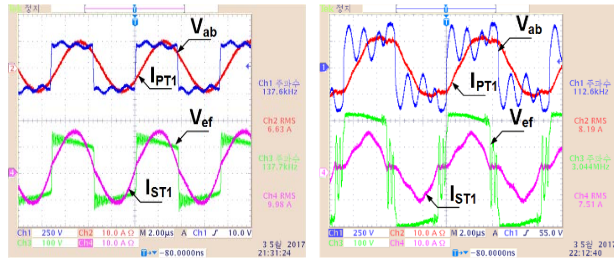

(a) Output ratings $100V_{DC}$/2kW, (b) Output ratings $190V_{DC}$/2kW
(ch1:250V/Div., ch2:10A/Div., ch3:100V/Div., ch4:10A/Div., 2us/Div.)
Figure11. Experimental waveforms of mode 1($100V_{DC} \sim 190V_{DC}$)

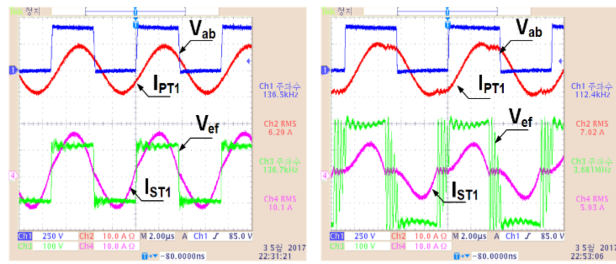

(a) Output ratings $200V_{DC}$/2kW, (b) Output ratings $390V_{DC}$/2kW
(ch1:250V/Div., ch2:10A/Div., ch3:100V/Div., ch4:10A/Div., 2us/Div.)
Figure 12. Experimental waveforms of mode 2 ($200V_{DC} \sim 390V_{DC}$)

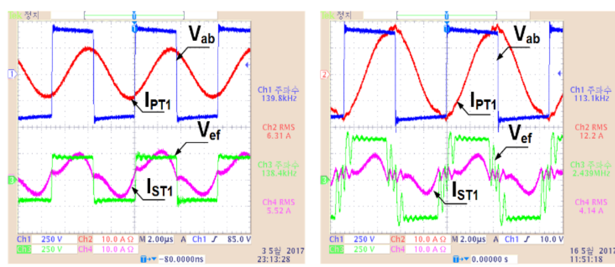

(a) Output ratings $400V_{DC}$/2kW, (b) Output ratings $800V_{DC}$/2kW
(ch1:250V/Div., ch2:10A/Div., ch3:250V/Div., ch4:10A/Div., 2us/Div.)
Figure 13. Experimental waveforms of mode 3 ($400V_{DC}$ to $800V_{DC}$)

Figure 10 shows the experimental waveforms of mode 0, whose output voltage ranges from $50V_{DC}$-$90V_{DC}$. Mode 0 could only be tested up to 900W because of the constraints of the gain characteristic curve. Figure 11, Figure 12 and Figure 13 respectively show the operating waveforms of mode 1 ($100V_{DC}/190V_{DC}$), mode 2 ($200V_{DC}/390V_{DC}$) and mode 3 ($400V_{DC}$ / $800V_{DC}$) for a 2kW load condition.
Figure 14 shows the output voltage (V_o), the output current (I_o), primary current (I_{PT1}) and voltage (V_{ab}) across the terminals of resonant circuit 1 as the converter transits from a lower operating mode to a higher operating mode. The proposed converter changes its operating mode from mode 0 to mode 1, whenever the output voltage (V_o) is greater than or equal to $110V_{DC}$. When the output voltage (V_o) is greater than or equal to $210V_{DC}$, the converter's operating mode changes from mode 1 to mode 2, and it transits from mode 2 to Mode 3 whenever the output voltage (Vo) is greater than or equal to $410V_{DC}$.

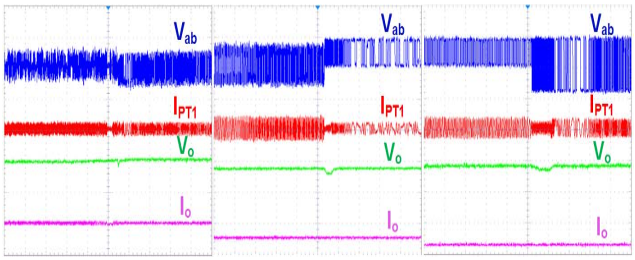

(a) Mode0⇒Mode1, (100V, 5A,40ms/Div) (b) Mode1⇒Mode2, (250V, 5A, 40ms/Div) (c) Mode2⇒Mode3 (500V, 5A,40ms/Div)

Figure 14. Experimental waveforms of the transformer primary voltage /current and the output voltage/current when the proposed converter transits from a lower operating mode to a higher mode.

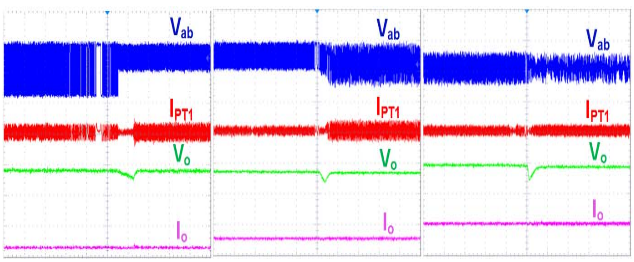

(a) Mode3⇒Mode2, (500V, 5A,40ms/Div) (b) Mode2⇒Mode1, (250V, 5A, 40ms/Div) (c) Mode1⇒Mode0 (100V, 5A,40ms/Div)

Figure 15. Experimental waveforms of the transformer primary voltage /current and the output voltage / current when the converter transits from a higher operating mode to a lower operating mode.

Figure 15 shows the output voltage (V_o), the output current (I_o), primary current (I_{PT1}) and voltage (V_{ab}) across the terminals of resonant circuit 1 as the converter transits from a higher operating mode to a lower operating mode. Whenever the output voltage (V_o) is less than or equal to $390V_{DC}$, the converter's operating mode transits from mode 3 to mode 2. When the output voltage (V_o) is less than or equal to $190V_{DC}$, the converter's operating mode changes from mode 2 to mode 1, and it transits to mode 0 whenever the output voltage is less than or equal to $90V_{dc}$.

As shown in Figure 16, a bandwidth is provided via programing to ensure stable mode transitions. Maximum efficiency characteristics are obtained in mode 2 for all output voltage and load conditions. A maximum efficiency of 96.42% is obtained with a 1.5kW load when the output voltage is $300V_{dc}$. However, an efficiency of 95.93% is obtained with a 2kW load, when the LLC converter operates with a controllable output voltage of $200V_{dc}$ and $300V_{dc}$. Figure 16 (a) shows the flow chart of the algorithm used to control the proposed converter.

V. CONCLUSION

An LLC resonant converter operating over a wide controllable output voltage ($50V_{DC}$~$800V_{DC}$) with high efficiency characteristics was presented. By changing the switching pattern of the primary switching devices, the converter can transit from one operating mode to the other and then control a wide output voltage range with minimum voltage and current over/under-shoots. Each mode operates at a varying frequency.

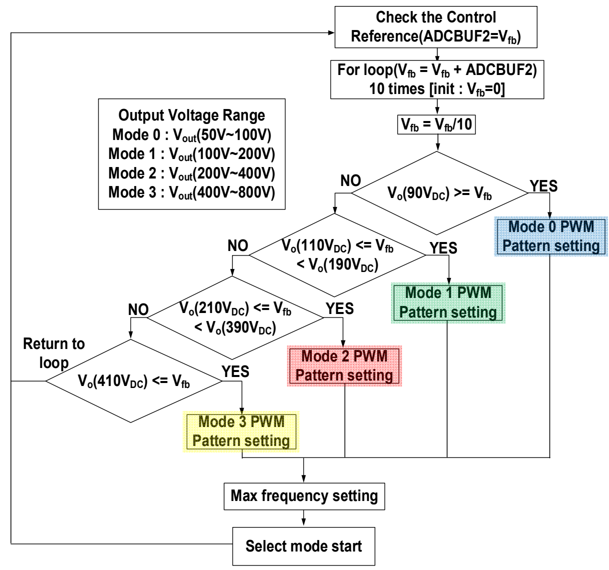

(a)

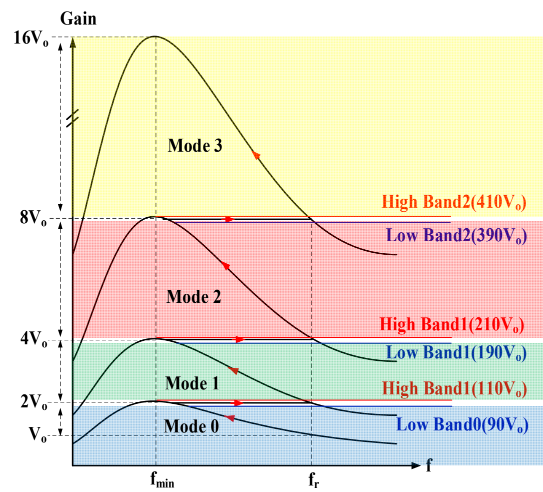

(b)

Figure 16. (a) Control flow chart and (b) gain characteristic of all operating mode of the proposed converter.

ACKNOWLEDGMENT

This work was supported by the Energy Technology Development Program of the Korea Institute of Energy Technology Evaluation and Planning (KETEP) granted financial resource from the Ministry of Trade, Industry & Energy, Republic of Korea (NO.20172020108500)

REFERENCES

[1] R. Beiranvand, B. Rashidian, M. R. Zolghadri, and S. M. H. Alavi, "Using LLC resonant converter for designing wide-range voltage source," IEEE Trans. Ind. Electron., vol. 58, no. 5, pp. 1746–1756, May 2011.

[2] J. Deng, C. C. Mi, R. Ma, and S. Li, “Design of LLC resonant converters based on operation-mode analysis for level two PHEV battery chargers,” IEEE Trans. Mechatronics, vol. 20, no. 4, pp. 1595–1606, Aug. 2015.

[3] Zhengyang Liu; Bin Li; Fred C. Lee; Qiang Li, “Design of CRM AC/DC converter for very high-frequency high-density WBG-based 6.6kW bidirectional on-board battery charger”, 2016 IEEE Energy Conversion Congress and Exposition (ECCE), pp1-8, 2016

[4] Najam ul Hassan, Yoon-Hae Kim, Byung-Moon Han, Jun-Young Lee “A Hybrid DC/DC Converter for EV OBCs Using Full-bridge and Resonant Converters with a Single Transformer”, Journal of Power Electronics, Vol. 17, No. 1, pp. 11-19, January 2017

[5] Haibing Hu, Xiang Fang, Oian Zhang, Z. John Shen, Issa Batarseh, “Optimal Design Considerations for a Modified LLC Converter with Wide Input Voltage Range Capability Suitable for PV Applications”, 2011 IEEE Energy Conversion Congress and Exposition, pp3096-3103, 2011.11

[6] Milan M. Jovanovic, Brian T. Irving, “On-the-Fly Topology-Morphing Control-Efficiency Optimization Method for LLC Resonant Converters Operating in Wide Input-and/er Output-Voltage Range”, IEEE Transactions on Power Electronics, Vol. 33, No. 3, pp2596-2608, March 2016

[7] Hongfei Wu; Xiaohai Zhan; Yan Xing, “Interleaved LLC Resonant Converter With Hybrid Rectifier and Variable-Frequency Plus Phase-Shift Control for Wide Output Voltage Range Applications”, IEEE Transactions on Power Electronics, Vol. 32, No. 6, pp 4246-4257, 2017

[8] Dong-Hyun Lee, Won-Il Choi, Chang-Pyo Hong, Hag-Wone Kim, Kwan-Yuhl Cho, “Carrier Comparison PWM Method of Vienna Rectifier for Reduction of Common Mode Voltage”, The Transactions of the Korean Institute of Power Electronics, Vol. 21, No. 2, pp. 126-133, April 2016

[9] Songhee Yang, Jin-Hyuk Park, Kyo-Beum Lee, “A Carrier-Based PWM with Synchronous Switching Technique for a Vienna Rectifier”, 2016 IEEE International on Power and Energy (PECon), pp. 728-733, 2016

[10] Eun-Soo Kim, “LLC resonant converter operating in wide input or output voltage range”, Korea Patent Application No. 10-2016-0149290, 2016. 11